



Research article

Interaction of eugenol-based anti-tuberculosis nanoemulsion with bovine serum albumin: A spectroscopic study including Rifampicin, Isoniazid, Pyrazinamide, and Ethambutol

Keerthana M^a, Parvathy Mohan Menon^b, George Priya Doss C^b, Chandrasekaran Natarajan^{a,*}

^a Centre for Nanobiotechnology, VIT University, Vellore-632014, Tamil Nadu, India

^b Department of Integrative Biology, School of Bio Sciences and Technology, VIT University, Vellore-632014, Tamil Nadu, India

ARTICLE INFO

Keywords:

Nanoemulsion
Tuberculosis
Fluorescence
Quenching
Eugenol oil

ABSTRACT

Tuberculosis (TB), a deadly infectious disease, is primarily caused by the bacterium *Mycobacterium tuberculosis*. The misuse of antibiotics has led to the development of drug resistance, prompting researchers to explore new technologies to combat multidrug-resistant Tuberculosis (MDR TB). Phospholipid-based nanotherapeutics, such as nanoemulsions, are gaining traction as they enhance drug solubility, stability, and bioavailability. Our study focuses on the interaction between Bovine Serum Albumin (BSA) and a drug-loaded nanoemulsion based on Eugenol. This nanoemulsion incorporates Eugenol, Clove, cinnamon oil, and first-line anti-tuberculosis drugs like Rifampicin, Isoniazid, Pyrazinamide, and Ethambutol. The primary objective is to assess the biosafety profile of the nanoemulsion upon interaction with BSA. We employed Fluorescence, UV-visible, and Fourier Transform Infrared Spectroscopy (FTIR) to analyze this interaction.

UV-visible spectroscopy detected changes in hydrophobicity due to structural alterations in BSA near the tryptophan residue, leading to the formation of ground-state complexes. Fluorescence spectroscopy demonstrated that the nanoemulsion effectively quenched fluorescence originating from tryptophan and tyrosine residues. Studies using synchronous and three-dimensional spectroscopy point to a potential modification of the aromatic environment of BSA by the nanoemulsion. Resonance light scattering spectra indicated the formation of large aggregates due to the interaction with the nanoemulsion. The second derivative FTIR spectra showed an increase in the magnitude of secondary structure bands, suggesting a conformational shift. This research has significant pharmacological implications for developing safer, more targeted drug delivery systems. The information obtained from the interaction of the nanoemulsion with the blood carrier protein is vital for the future development of superior carriers with minimal adverse effects on patients. It is crucial to remember that conformational changes brought on by drug-ligand complexes attaching to carrier proteins may have negative consequences. Therefore, this study enhances the in vitro evaluation of potential adverse effects of the nanoemulsion on serum proteins.

* Corresponding author.

E-mail addresses: nchandra40@hotmail.com, nchandrakaran@vit.ac.in (C. Natarajan).

<https://doi.org/10.1016/j.heliyon.2024.e28306>

Received 31 October 2023; Received in revised form 15 March 2024; Accepted 15 March 2024

Available online 19 March 2024

2405-8440/© 2024 Published by Elsevier Ltd.

This is an open access article under the CC BY-NC-ND license

(<http://creativecommons.org/licenses/by-nc-nd/4.0/>).

1. Introduction

Tuberculosis (TB) is a communicable illness caused by *Mycobacterium tuberculosis*, an aerobic, rod-shaped, acid-fast bacilli that can thrive within macrophages [1]. As per the Global Tuberculosis Report 2022, it has been reported that 5.8 million newly diagnosed TB cases have had a significant impact on the statistics. This led to an increase in the number of TB fatalities that went untreated, as well as increased transmission in the community and the prevalence of TB among individuals [2]. Since *Mycobacterium tuberculosis* forms a reservoir in the alveolar macrophages and it is difficult for anti-TB medications supplied systemically to reach the lungs or alveoli, several medicines are now being tested in clinical trials to overcome drug resistance [3]. Currently, available first-line anti-tubercular drugs must be taken long-term to treat TB, which occasionally results in patient non-compliance and the establishment of multidrug-resistant strains known as XDR-TB (Extensively Drug Resistant TB) and MDR TB (Multi Drug Resistant Tuberculosis).

This necessitates the development of innovative technologies and strategies to combat this resistance. One approach is to enhance the delivery of antibiotics to the target organ or tissue without compromising their potency or efficacy, thereby increasing the therapeutic index of the drug, making harsh chemotherapy more tolerable, and reducing systemic side effects can be attained using nanotechnology-based drug repurposing method [4–6]. Nanotechnology in drug delivery allows for drug encapsulation, improving solubility and preventing degradation. It also enhances epithelial absorption, prolongs circulation time in the body, enables targeted drug delivery to a specific tissue or organ, controls drug release, and facilitates cellular uptake of the drug [7–10]. On the contrary, Nanoparticles adhere to any aspect of the microbe and act as a storehouse for the enclosed drugs taken up by infected cells, enhancing the accessibility of the drug and circumventing resistance to it [11,12]. Nanotechnology-based medicine aids in eliminating drug-resistant bacteria by binding to their membrane. Liposomes' membrane-like structure allows them to merge with bacterial walls and pump substantial amounts of drugs into their cytoplasm, thereby overwhelming the drug efflux pumps.

Considering their many advantages, such as ease of production, higher drug loading capacity, improved drug dissolution, and bioavailability, reduced patient variability, controlled drug release, and resistance to enzymatic degradation, essential oil-based nanoemulsions hold particular promise for the delivery of poorly water-soluble drugs [13,14]. It is well-informed that nanocarrier biosafety is essential for drug delivery systems. Hence, it is essential to investigate in vitro behavior to understand the possible toxicity of nano-drug delivery systems aided by research into how they interact between nanocarriers and biomolecules [15]. As the most effective route for drugs or drug carriers to reach their site is over blood circulation, it is important to understand the interaction of these substances with proteins in the blood [16]. One of the bloodstream's transporter proteins, serum albumin, is used to analyze the prepared nanoemulsion biosafety and provide a more effective medication delivery method.

Serum protein, a vital class of biomacromolecules, consists of one or more elongated chains of amino acid residues and plays diverse roles within cells. These roles include responding to stimuli, providing structural support to cells and organisms, aiding in metabolic processes, transporting molecules, and catalyzing biochemical reactions. Loss of protein quality can lead to various health complications in the body. Efforts are underway to develop more efficient methods for studying the relationship between protein structure and function and designing effective drugs. Among proteins, Bovine serum protein (BSA) stands out as one of the most common water-soluble proteins, renowned for its role in transporting fatty acids, anions, and other amphiphilic molecules in the bloodstream. The primary structure of BSA consists of 9 loops connected by 17 disulfide bonds. It comprises 3 domains (I, II, and III), each containing two sub-domains (A and B). BSA is well-characterized with a molecular weight of 66.4 kDa and 583 amino acid residues, featuring a spherical, heart-shaped and a pI value of 4.9. BSA contains Tryptophan (TRP) residues at TRP-134 and TRP-213 [17]. Due to its surface composition rich in charged amino acids, this protein exhibits high binding affinity for various small compounds, making it a subject of extensive research. Pioneering work by Sudlow et al., in 1975 highlighted the significant binding affinity of serum albumins, including BSA, for medications and small compounds, particularly at sites such as sites I and II. These proteins are crucial in transporting drugs in the bloodstream [18].

The present focus in biomedical research is studying the interaction between nanotechnology-based drug carriers and proteins to learn more about the potential structural alterations that may result from it. Therefore, a variety of spectroscopic techniques were used, including fluorescence spectrophotometry and UV-visible spectrophotometry, which assess the nanoemulsion protein interaction in conjunction with potential variations in the aromatic residue environment, FTIR, and which assess changes in secondary structural conformations [19–21]. Additionally, the current study is anticipated to shed light on the implications of biosafety on pharmacology and the biological and therapeutic effects of drugs loaded into eugenol-based nanoemulsions. This study presents a convincing argument for the impact of nanophase drug delivery on the body's carrier protein. As a result, this finding has important implications for pharmacology, particularly in creating more safe and precisely focused drug delivery systems that pose less risk. The results obtained here from the interaction of the novel drug-carrier system, a nanoemulsion, with the blood carrier protein are therefore important information for the design of better carriers with lower side effects for patients in the future since drugs made with ligands for binding to transport proteins can cause conformational modifications that may have negative effects. As an expected outcome, this study shall be further extended towards the molecular docking studies and in-vivo evaluation of its anti-TB activity in a suitable animal model which can reveal the biosafety profile of the nanoemulsion.

2. Materials and methods

This section provides all the spectroscopy methodologies for studying the interaction between BSA and eugenol-based drug-loaded nanoemulsion.

2.1. Materials

BSA (Bovine Serum Albumin) was obtained from HIMedia Laboratories Pvt. Ltd., Mumbai. Phosphate buffer saline of pH 7.4 was prepared in the lab using analytical-grade chemicals. 1st line anti-TB medications, including such as Rifampicin, Ethambutol dihydrochloride, Pyrazinamide, and Isoniazid were all acquired from HIMedia Laboratories Pvt. Ltd. in Mumbai. Sigma-Aldrich Chemicals Pvt Ltd, based in Bengaluru, supplied the essential oils clove, cinnamon leaf, and eugenol, as well as the non-ionic surfactants Tween 20 and Tween 80. High-quality, analytical-grade chemicals were used. All tests were conducted with Milli-Q water (Millipore Corporation).

2.2. Nanoemulsion preparation

Menon et al. optimized and formulated stable eugenol-based anti-Tb drugs loaded nanoemulsion using a pseudo ternary phase diagram and response surface methodology (RSM) [22]. For this study, we have prepared a stable Eugenol-based drug-loaded nanoemulsion as per the above-mentioned published literature where an optimized oil-to-water ratio was found to be 1:5. Eugenol-based three individual oil-in-water nanoemulsion was prepared using clove oil, cinnamon oil, and Eugenol respectively. Tween 80 was used as a surfactant for the eugenol nanoemulsion, while Tween 20 was used for the clove and cinnamon oil nanoemulsion. Nanoemulsions were prepared using 4.5% oil and 22% detergent with 8 min of probe sonication at 40% strength, with a 30-s pulse every 2 min at a temperature of 4 °C. In the case of nanoemulsion loaded with anti-TB drugs, all four anti-TB drugs (Rifampicin, Isoniazid, Pyrazinamide, and Ethambutol) were added at a concentration of 1 mg/ml. The created nanoemulsion was stored overnight to check for phase separation. It is then further characterized to find out its stability and size.

2.3. Characterization of the prepared nanoemulsion

As nanoemulsions are thermodynamically unstable, it is necessary to prove the stability of the prepared nanoemulsion through evaluations like kinetic stability, DLS particle size, PDI, and zeta potential analysis.

2.3.1. Thermodynamic stability studies

Stability is the primary barrier to the expanding use of nanoemulsions. The Ostwald ripening process has been observed to potentially harm nanoemulsions, limiting their applicability despite the widespread belief that these systems may remain stable for years. This is because of the tiny droplet size. A kinetic stability study is usually performed to check the propensity to split off into the component phase [23]. Because of instability processes, including creaming, coalescence, flocculation, Ostwald ripening, and phase separation, nanoemulsions are thermodynamically unstable systems that may experience structural changes during an extended storage period. Over time, the kind of surfactant used in nanoemulsion proved to be critical for thermodynamic stability. This feature can be connected to many surfactant characteristics, including their capacity to reduce interfacial tension and chemical structure. This characteristic seems to have an indirect connection to the stability of the nanoemulsion. Hence, it is necessary to perform the kinetic stability study to check the stability of the prepared nanoemulsion [24]. Through centrifugation and temperature experiments, the kinetic stability of the nanoemulsion was investigated. Specifically, the nanoemulsion was heated to 45 °C, cooled to 4 °C, and then allowed to rest at room temperature for two days in three cycles. After conducting temperature tests, the physical stability of these emulsions was confirmed by centrifuging them at 1500×g for 30 min.

2.3.2. Measurement of size, PDI, and zeta potential

Using the SZ-100 Horiba nanoparticle analyzer, the dynamic light scattering (DLS) method was used to evaluate the nanoemulsion droplet size (nm), and the polydispersity index (PDI). Using Milli-Q, nanoemulsion samples were diluted to a 1:3 ratio. Additionally, samples were analyzed in a transparent zeta cell, and the SZ-100 Horiba nanoparticle analyzer was used to calculate the Zeta potential. Nanoemulsion droplet size, PDI, and Zeta potential were measured at 25 ± 1 °C [22].

2.4. Stock solutions and sample preparation

A fixed concentration of BSA (1 mg/ml) is freshly prepared with Phosphate buffer saline of pH 7.4 and used as a control in all experiments. Five different dilutions of each eugenol-based drug-loaded nanoemulsion (Eugenol, Clove, and Cinnamon) with a 50 μ L increase in concentration (50, 100, 150, 200, 250 μ L) were interacted with a freshly prepared BSA solution and kept for incubation at room temperature for 30 min. The interacted samples were further investigated with UV-visible spectroscopy, Fluorescence spectroscopy, and FTIR.

2.4.1. UV-visible spectroscopy

A double-beam UV-visible spectrophotometer (Jenway® 6850 Spectrophotometer from Antylia Scientific) with a resolution of 0.1 nm was used to measure absorbance. BSA and its interacting samples. UV-visible spectra from 190 to 600 nm were recorded.

2.4.2. Analysis of fluorescence quenching

Non-fluorescent complex formation was the cause of the fluorescence quenching effect. When excited state processes, energy transfer, ground-state complex formation, and collisional quenching occur in combination with other chemical interactions, the

fluorescence quantum yield from a fluorophore decreases, and a phenomenon known as fluorescence quenching occurs. Proteins are thought to possess inherent fluorescence, mostly from Tryptophan, tyrosine, and phenylalanine residues. Its intrinsic fluorescence frequently varies in response to the concentration of the ligand during their interactions. As a result, fluorescence may be considered a method for determining how ligands and proteins interact [25]. Throughout the experiment, the concentrations of nanoemulsion were changed while the concentrations of BSA solutions were maintained constant. A Fluoro Spectrophotometer (Jasco FP-8300) equipped with a quartz cuvette (10 mm path length) was used to measure the fluorescence quenching. Bandwidths for excitation and emission were held constant at 2.5 and 5 nm. The emission maxima of BSA have been identified in the spectral region of 285–400 nm in both the presence and absence of the eugenol-based drug-loaded nanoemulsion, at an excitation wavelength of 279 nm and a scan speed of 500 nm/min. The quenching percentage of the interacted system was calculated using the below-mentioned formula [26].

$$\text{Quenching Percentage} = [(I_0 - I)/I_0] * 100 \%$$

2.4.3. Synchronous fluorescence spectra

Synchronous fluorescence spectra aid in seeing fluorescence quenching, peak shifting, and conformational changes in BSA when tryptophan or tyrosine residues are altered. Tryptophan and tyrosine residues indicate the molecular environment surrounding the chromophores, and synchronous fluorescence spectra offer information on this environment when the wavelength interval ($\Delta\lambda$) between the excitation and emission wavelengths is between 15 and 60 nm [27]. By simultaneously scanning the emission and excitation monochromators using a Fluoro Spectrophotometer (Jasco FP-8300) fitted with a quartz cuvette (10 mm path length), synchronous fluorescence spectra were generated. A conformational change around BSA could be observed when the wavelength interval ($\Delta\lambda$) 15 for tyrosine residues is 60 nm for tryptophan residues. Bandwidths for excitation and emission were held constant at 2.5 and 5 nm with $\Delta\lambda$ values of 15 and 60 nm. 200 nm–400 nm were fixed as excitation start and end wavelengths with 500 nm/min as scan speed.

2.4.4. Resonance light scattering spectra (RLS)

Resonance light scattering spectra (RLS) indicate complex formation aggregation states between protein and the ligand. Rayleigh scattering at a wavelength close to or at the scattering molecules' absorption bands is known as resonance light scattering (RLS), and it can provide strong signals and good selectivity [28]. RLS generation is associated with creating certain aggregates, and the dimensions of the aggregate generated in solution are the primary determinant of RLS intensity. Considering these aspects, an interpretation from RLS spectra would reveal the interaction with BSA when scanning in the synchronous mode in the 200 nm–800 nm range $\Delta\lambda$ at 0 [29]. Using a Fluoro Spectrophotometer (Jasco FP-8300) with a quartz cuvette (10 mm path length), resonance light scattering spectra were acquired by simultaneously scanning the emission and excitation monochromators in a synchronous mode in the wavelength range of 200 nm–800 nm by fixing the $\Delta\lambda$ at 0 nm. Excitation and emission bandwidths were maintained at 5 nm, with a scan speed of 500 nm/min.

2.4.5. Three-dimensional fluorescence spectra

Utilizing a quartz cuvette (10 mm path length) and a Fluoro Spectrophotometer (Jasco FP-8300), three-dimensional fluorescence spectra of the interacting samples were measured. The measurement type remains a 3D scan, and emission was chosen as the data mode. The wavelengths of excitation and emission were adjusted to 200 nm and 900 nm. The medium sensitivity sample intervals for excitation and emission were set at 5 and 0.5 nm respectively. The excitation and emission bandwidth were set at 5 nm, while the scan speed remained at 5000 nm/min.

2.4.6. Fourier Transform Infrared Spectroscopy

FTIR spectroscopy is one of the most widely utilized methods for evaluating proteins and peptides. The repeating amino acid building blocks that make up the structure of proteins and peptides yield many distinct infrared absorption bands or amide bands. These bands communicate structural and chemical data. As a result, FTIR is frequently used to examine and characterize protein secondary structures [30,31]. FTIR-ATR analysis can detect a change in the secondary structure of a protein by interpreting the visible modification in their fingerprint amide region when an interaction occurs. Conformational changes show increased or decreased bands of α -helix, β -sheets, β -turns, and random coils, providing significant insights into the protein interaction with nanoemulsion [32].

FTIR-ATR analysis was carried out using Jasco FT/IR 6800 with 4 cm⁻¹ resolution to investigate the influence of a eugenol-based drug-loaded nanoemulsion on the secondary structure of BSA. Freshly produced BSA (1 mg/ml) was incubated for 30 min at room temperature with a eugenol-based drug-loaded nanoemulsion. FTIR spectra of 4000 to 400 cm⁻¹ with 512 scans were recorded for each spectrum. A second derivative of the FTIR spectrum was created using OriginLab 2016 to decode the limited alterations emerging in the BSA's amide I region of the spectrum following the eugenol-based nanoemulsion binding.

3. Results and discussion

3.1. Characterization of prepared eugenol-loaded nanoemulsion

The optimized eugenol-based drug-loaded nanoemulsion undergoes characterization to ensure that the nanoemulsion is stable and within the defined size range, as mentioned in our previous study [22]. Nanoemulsion stability was assessed through overnight

incubation, heating and cooling cycles, and centrifugation. During the overnight incubation period, these formulations showed no phase separation, and no precipitation was observed during three repeated heating and cooling cycles followed by centrifugation. No phase separation or precipitation was observed, indicating stability. From the DLS, it can be confirmed that the prepared nanoemulsion showed a slight increase in size compared to the free nanoemulsion due to different drugs incorporated into the nanoemulsion systems. The same phenomenon was also seen in the cited literature, where the droplet size of nanoemulsion increased in addition to different amounts of curcumin [13]. The nanoemulsions produced for cinnamon oil, clove oil, and Eugenol produced had typical droplet sizes between 10 and 20 nm. All nanoemulsions had Polydispersity index (PDI) values less than 0.5, which denotes the level of homogeneity inside the nanoemulsion; a lower PDI value denotes a higher degree of homogeneity. Literature reveals that a PDI of 0.3 indicated homogeneity in the case of a liposome or Nano formulation [33]. Nanoemulsion stability and accumulation probability are assessed by measuring the electric charge on the emulsion's surface. Nanoemulsion may keep their shape and size due to the strong surface charges that generate repulsion between adjacent surfaces. All of the emulsions had values that were relatively small, negative, and in the middle of the range when the charges were measured using the zeta potential. This suggests using of a non-ionic emulsifier that encapsulates the entire particle, creating a certain force between the oil and water and acting as a barrier to prevent agglomeration. Additionally, it is also clear from the literature that the non-ionic surfactants' hydrophobic group causes the zeta potential to decrease to a smaller, negative value [13]. The conclusion on eugenol-based drug-loaded nanoemulsion is mentioned in Table 1.

3.2. Protein interaction studies

3.2.1. UV-visible spectroscopy studies

UV-visible spectroscopy was used to investigate the protein interaction with the ligand. Typically, the aromatic milieu surrounding the amino acid residues determines the molecular shape of proteins. Biomolecules' interactions with their immediate environment immediately cause variations in their UV-visible spectra [34].

Our study investigated the impact of a different eugenol-based drug-loaded nanoemulsion concerning the absorption spectrum of BSA protein. BSA of 1 mg/ml concentration interacted with a series of 5 dilutions of Eugenol-based drug-loaded nanoemulsion with a 50 μ L increase in concentration. As depicted in Fig. 1, BSA shows absorption peaks at 215 nm and 279 nm, where 215 nm stands for the protein's peptide backbone π - π^* transition, and a less intense peak at 279 nm represents the aromatic amino acids of protein, i.e., Tryptophan, Tyrosine, and Phenylalanine [35–37].

The spectra of BSA, in addition to all eugenol-based drug-loaded nanoemulsions such as Eugenol, Clove, and Cinnamon, showed an increase in absorption intensity and a bathochromic shift (redshift) in the absorption maxima revealed a variation in polarity pertinent to the tryptophan residue and the conformation changes in peptide strand of BSA. As a result, the detected fluctuation in hydrophobicity indicated a structural modification of BSA near tryptophan residue, and ground-state complexes were formed [35].

The disturbance in absorption intensity at 215 nm is due to the polar solvent, such as PBS or water. This lessens the energy states of π - π^* electron cloud, thereby experiencing a bathochromic shift [37].

As the EDLNE and CLDLNE concentration increases, the maxima peak at 279 nm drastically undergoes a bathochromic (red) shift of 340 nm as represented in Fig. 1 a and Fig. 1 b respectively. In contrast, CNDLNE also shows a similar shift with a less intense peak maxima as shown in Fig. 1 c. It is surprising to learn that the hyper-chromic effect that is achieved is caused by the adhesion between the BSA molecule to the outer surface of a nanoemulsion with a smaller size and an enhanced surface area. The BSA molecules and the nanoemulsion form a ground state complex concerning changes in their hydrophobicity or polarity around tryptophan moieties [34]. As reported by Zadymova et al. absorption spectra of tween 80 on interaction with BSA showed a bathochromic and hyperchromic shift, whereas tween 20 showed only a bathochromic shift in evidence with our results. This is due to their ground state complex formation through hydrogen bonding between Tween and BSA polar moieties [38,39]. Researchers studied human serum albumin interaction with Cinnamaldehyde and also showed increased absorption intensity of the UV absorption spectra [40]. LI Jin-zhi, LIU Chang-jin, SHE Zhi-yu et al. also reported a similar interaction when BSA interacted with eugenol [41].

Further, many works of literature support the results obtained through UV absorption spectra, where BSA, upon interacting with the anti-TB drug, showed an increase in their absorption spectra intensity on their increasing concentration [42–45]. The referred literature shows that the interaction between nanoemulsion (quencher) and BSA formed a ground state complex formation. Hence, interaction with nanoemulsion led to increased absorption intensity and a redshift, suggesting structural modifications.

3.2.2. Fluorescence spectra studies

Fluorescence spectroscopy is a useful technique for determining protein-ligand interactions [46]. BSA exhibits an endogenous

Table 1

Characterization of prepared Eugenol-based drug-loaded nanoemulsions and their code used in the present article.

Nano Emulsion Type with its code	Overnight Incubation	Temperature & Centrifugation studies	Mean Droplet Size (nm)
ENE - Eugenol nanoemulsion	No Phase separation	Stable	11.2
EDLNE - Eugenol drug-loaded nanoemulsion	No Phase separation	Stable	17.4
CLNE - Clove nanoemulsion	No Phase separation	Stable	11.9
CLDLNE = Clove drug-loaded nanoemulsion	No Phase separation	Stable	13.6
CNNE - Cinnamon nanoemulsion	No Phase separation	Stable	9.9
CNDLNE - Cinnamon drug-loaded nanoemulsion	No Phase separation	Stable	12.9

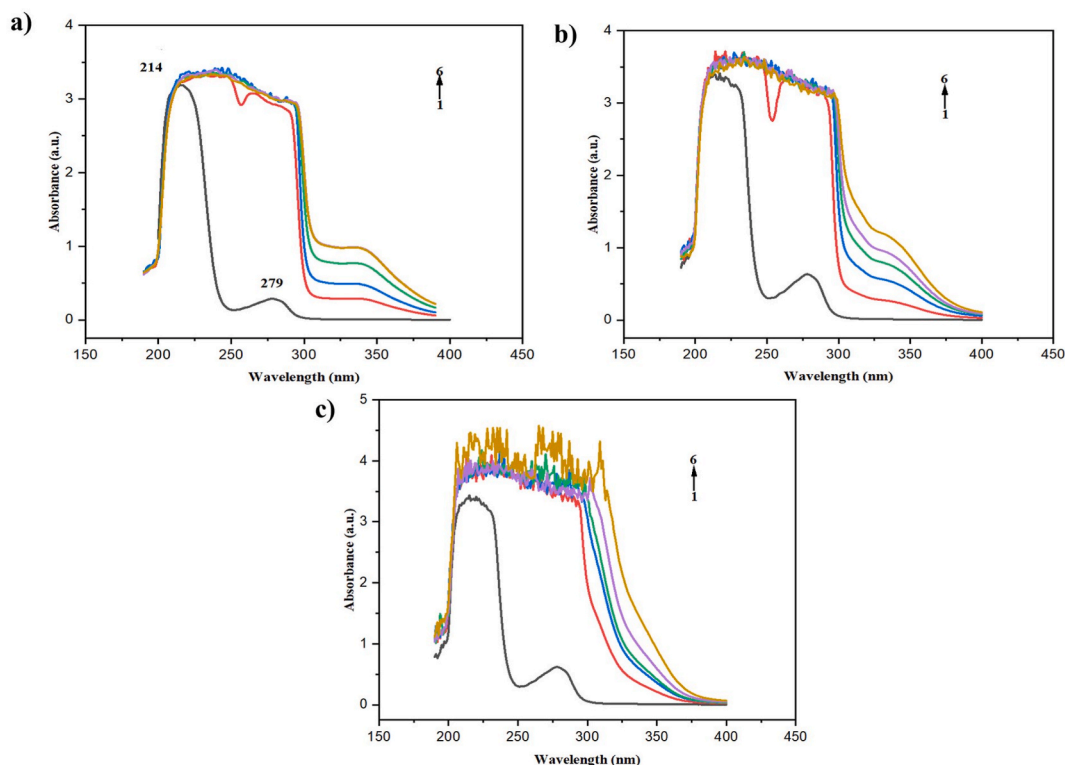


Fig. 1. UV-Visible absorption spectra of BSA, $c(\text{BSA}) = 1 \text{ mg/ml}$ and its interaction with a) Eugenol Drug loaded nanoemulsion, b) Clove Drug loaded nanoemulsion, c) Cinnamon Drug loaded nanoemulsion, where the concentration $c(\text{EDLNE}) = c(\text{CLDLNE}) = c(\text{CNDLNE}) = 5$ different dilution with a $50 \mu\text{L}$ increase in concentration (50, 100, 150, 200, 250 μL).

fluorescence because it is rich in Tryptophan, tyrosine, and phenylalanine. In particular, Tryptophan in BSA contributes more to intrinsic fluorescence than tyrosine and phenylalanine, thereby being extensively used to investigate Ligand-BSA interactions [47]. Trp 134 and Trp 213 are the two tryptophan residues present in BSA, whereas the former is located in domain I A (hydrophilic region) and later in domain II A (hydrophobic region). Due to its ionization, Phenylalanine holds a low quantum yield and tyrosine quenching. Therefore, the intrinsic fluorescence is highly susceptible to changes in the Tryptophan and its surrounding environment [48], while the changes are due to the transition of protein conformation, association of subunit, substrate interaction, or degradation [49]. We utilized fluorescence quenching, which can happen in many ways, including excited-state reactions, molecular rearrangements, energy transfer, ground-state complex formation, and collisional quenching, to examine the effects of a drug-loaded eugenol nanoemulsion on BSA protein in our study [50].

After excitation at 279 nm, emission spectra of BSA in the presence of Eugenol-based nanoemulsion -EDLNE, CLDLNE, and CNDLNE provided strong emission maxima of BSA at 339 nm, which mostly comes from excitation of tryptophan residue, Trp 213 present at the hydrophobic pocket of domain II as depicted in Fig. 2 a, Fig. 2 b and Fig. 2 c respectively. It is generally recognized that tryptophan residues buried in hydrophobic environments produce a fluorescence Peak of emission at 340–345 nm (shorter wavelength), While tryptophan residues on the outermost layer and accompanied by a higher hydrophilic milieu exhibit an emission maximum at longer wavelength [19,51]. Hence, it can be said that our nanoemulsion system interacted with Trp 213 present at the hydrophobic pocket of domain II.

When increasing the concentration of nanoemulsion added to BSA, intrinsic fluorescence emission was found to be decreasing along with a discernible blue shift from 339 nm to 313 nm, suggesting a loss in polarity, an increase in hydrophobicity surrounding Tryptophan, and protein folding occurs most likely due to the loss of intricate structure of Trp 213 present in the domain II of hydrophobic core [27,52]. The quenching percentage of the interacted system was calculated using the below-mentioned formula [26].

$$\text{Quenching Percentage} = \left[\frac{I_0 - I}{I_0} \right] * 100 \%$$

The quenching percentages of BSA- EDLNE, BSA – CLDLNE, and BSA – CNDLNE were 99 %, 68.48 %, and 87.91 %, respectively. As a result of this strong quenching, it can be inferred that the binding of BSA on the surface of the nanoemulsion prompted the tertiary structure to change into a less compact structure as an outcome of nanoemulsion permeation into their hydrophobic cavity, which increases the hydrophobicity and modifies the aromatic milieu and lessens the polarity of the microenvironment surrounding the Trp-213 residue. Hence, nanoemulsion induced a strong quenching effect on BSA intrinsic fluorescence, indicating structural changes. Interaction primarily occurred with Trp 213 in the hydrophobic pocket of domain II.

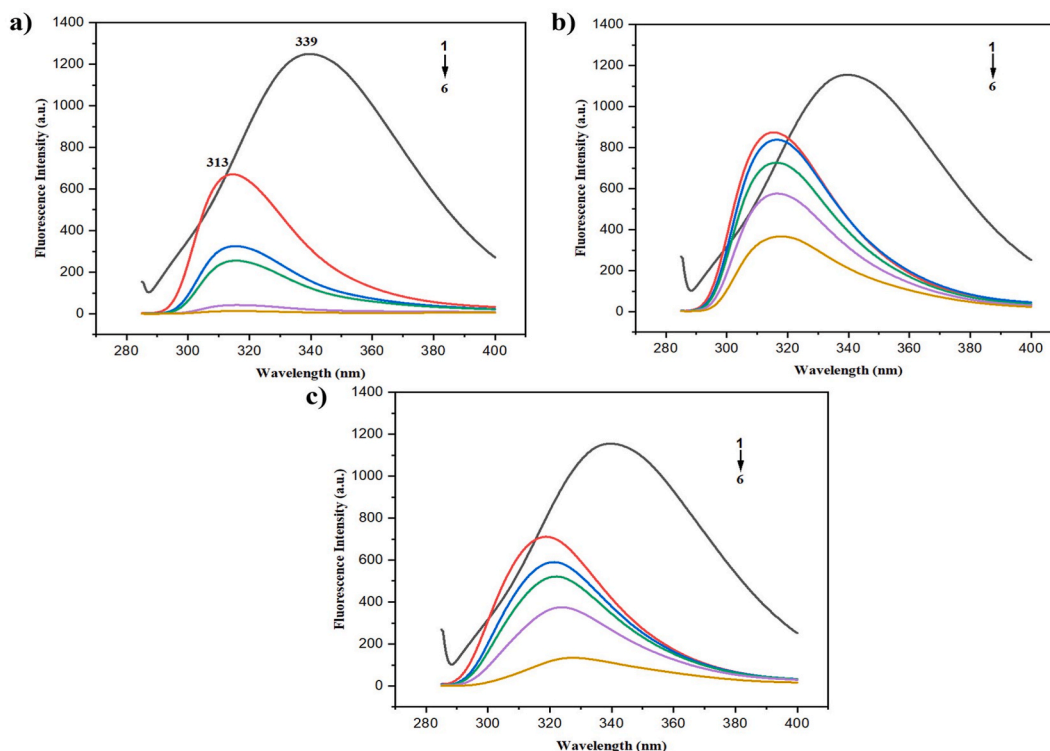


Fig. 2. Fluorescence emission spectra of BSA, $c(\text{BSA}) = 1 \text{ mg/ml}$ and its interaction of a) Eugenol Drug loaded nanoemulsion, b) Clove Drug loaded nanoemulsion, c) Cinnamon Drug loaded nanoemulsion, where the concentration $c(\text{EDLNE}) = c(\text{CLDLNE}) = c(\text{CNLNE}) = 5$ different dilution with a $50 \mu\text{L}$ increase in concentration (50, 100, 150, 200, 250 μL).

3.2.3. Synchronous spectra studies

By detecting the emission wavelength shift, synchronous fluorescence spectroscopy can reveal details regarding the milieu surrounding BSA's tryptophan and tyrosine residues. Any change or variation in the emission maxima location correlates to variations in polarity surrounding the chromophore molecule, i.e., Tryptophan, Phenylalanine, and Tyrosine. Modification in tyrosine and tryptophan residues of proteins is detected when the D-value between excitation and emission wavelengths is set to 15 and 60 [19].

As can be seen in Fig. 3, the synchronous spectra of BSA were obtained in the presence and absence of Eugenol-based nanoemulsion (EDLNE, CLDLNE, CNLNE) at D-values of 15 nm and 60 nm. It can be observed that the peak maxima at tyrosine residues are at 299 nm, which got red-shifted to 312 nm and decreased fluorescence intensity when interacted with increasing concentrations of EDLNE. In the case of Tryptophan, peak maxima were found at 339 nm in context with fluorescence spectra, which got blue shifted to 320 nm and decreased fluorescence intensity when interacted with increasing concentration of EDLNE as seen in Fig. 3 a and Fig. 3 b.

However, in the case of CLDLNE as shown in Fig. 3 c to Fig. 3 d, and CNLNE as shown in Fig. 3 e to Fig. 3 f, it was observed that the Tryptophan predominately involved in the interaction with respective nanoemulsion was much stronger than the tyrosine residue, which can be evident. The results suggest that CNLNE and CLDLNE show decreased fluorescence intensity with the prominent blue shift from 340 nm to 319 nm and 325 nm, indicating a strong interaction with tryptophan moieties. In contrast, a weak or null interaction with tyrosine was observed as having a D-value of 15 nm spectra showing no quenching in CLDLNE, and a slight quenching starts at increasing concentration. A similar case was observed in many studies, where the tyrosine moieties interact very weakly with their respective ligand [53].

This significant shift (both red and blue) in the synchronous fluorescence spectra of tyrosine and tryptophan residues shows that molecular alteration surrounding the residues occurs, resulting in a more polar environment (less hydrophobic) around tyrosine and less polar environment (more hydrophobic) around Tryptophan in context with the intrinsic fluorescence spectra (Fig. 2). However, it is evident from the cited literature that on the increasing concentration of Tween 20, tryptophan residues in BSA moved to the more hydrophobic milieu, indicating that the CNLNE and CLDLNE nanoemulsion system undergoes most of its interaction in the tryptophan residue present in the hydrophobic cavity [39]. Further, Synchronous spectra revealed red and blue shifts, indicating changes in polarity around tryptophan and tyrosine residues. Hence, the obtained synchronous spectra reveal that the fluorescent quenching takes place strongly around Tryptophan rather than tyrosine, indicating the optimal interaction between BSA and the nanoemulsion system.

3.2.4. Resonance light scattering spectra (RLS) studies

RLS is an easy-to-use, quick, and sensitive technique for using a fluorescence spectrophotometer to analyze macromolecule

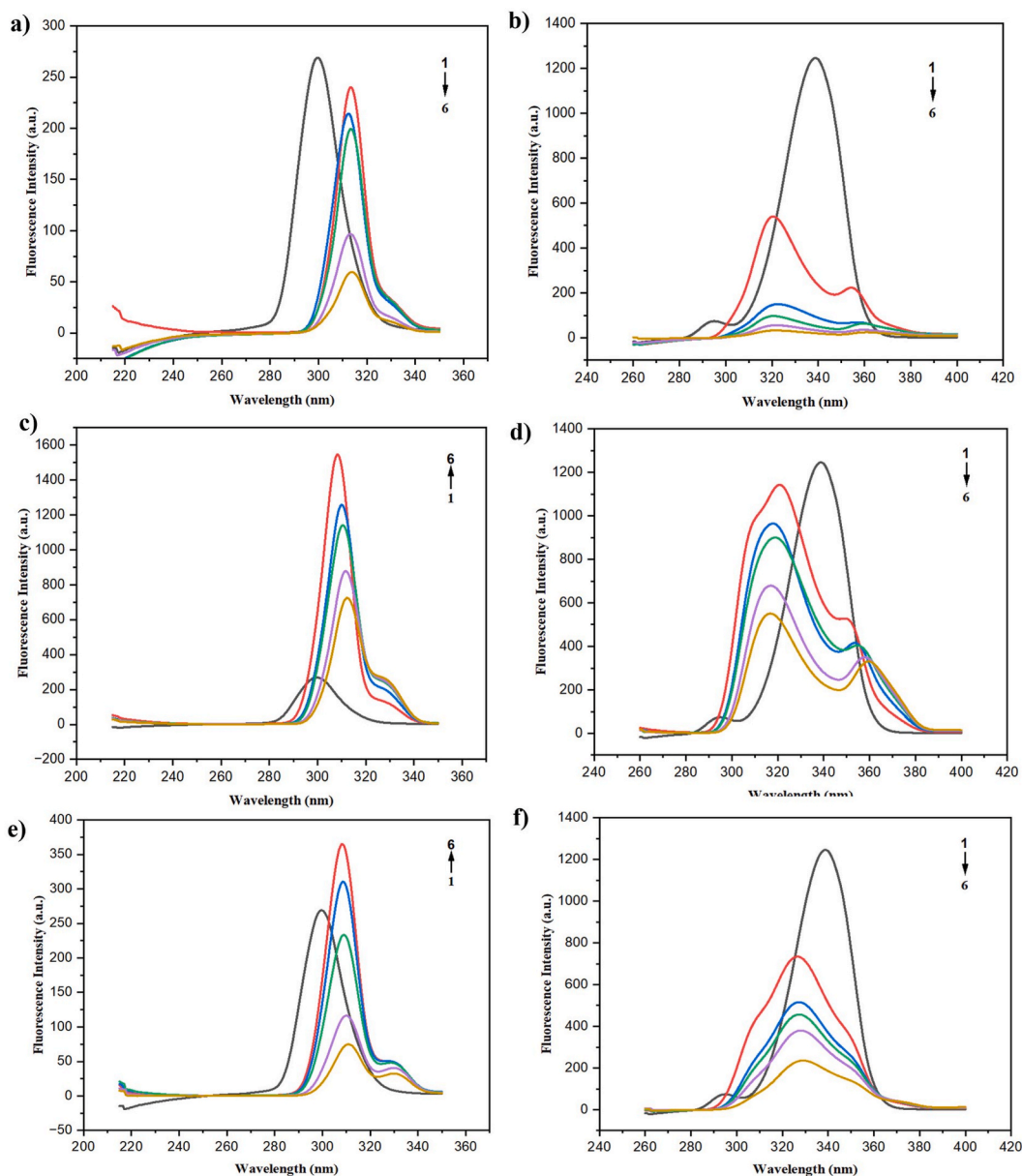


Fig. 3. Synchronous spectra of BSA, $c(\text{BSA}) = 1 \text{ mg/ml}$ and its interaction of a) & b) D-value of 15 nm and 60 nm of Eugenol Drug loaded nanoemulsion, c) & d) D-value of 15 nm and 60 nm of Clove Drug loaded nanoemulsion, e) & f) D-value of 15 nm and 60 nm of Cinnamon Drug loaded nanoemulsion, where the concentration $c(\text{EDLNE}) = c(\text{CLDLNE}) = c(\text{CNLNE}) = 5$ different dilution with a $50 \mu\text{L}$ increase in concentration (50, 100, 150, 200, 250 μL).

scattering signals. This method was used to investigate how BSA's size, shape, and structure change when it forms a complex with nanoemulsion [54]. As depicted in Fig. 4, the RLS peak intensity of protein increased when interacting with the nanoemulsion. This is due to the aggregation of BSA and our prepared nanoemulsion [51,52], and a larger aggregate dimension was formed in the solution [55]. Significantly, EGDLINE showed a maximum increase in peak intensity when compared to the other two. Therefore, RLS peak intensity increased, indicating BSA aggregation onto the nanoemulsion surface.

3.2.5. Three-dimensional fluorescence spectra

Additional information on the conformation of biomolecules in complexes with exogenous ligands may be gathered from the three-dimensional spectra of proteins. It assesses potential alterations in the Trp and Tyr residues and the aromatic milieu of BSA [56]. The 3D color plot was used in this work to express the 3D spectra of BSA and its interaction with Eugenol-based drug-loaded nanoemulsion. From Fig. 5, It was found that 3D spectra of BSA show Peak a, Peak 1, and 2, where Peak a is associated with the initial Rayleigh

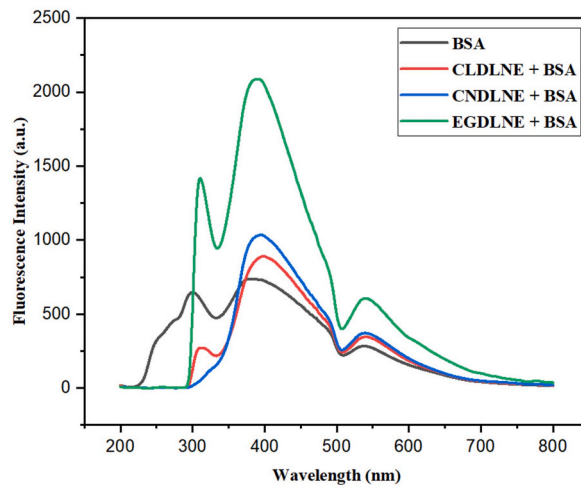


Fig. 4. Resonance Light Scattering Spectra of BSA, $c(\text{BSA}) = 1 \text{ mg/ml}$ and its interaction of Eugenol Drug loaded nanoemulsion, Clove Drug loaded nanoemulsion, Cinnamon Drug loaded nanoemulsion, where the concentration $c(\text{EDLNE}) = c(\text{CLDLNE}) = c(\text{CNDLNE}) = 250 \mu\text{L}$.

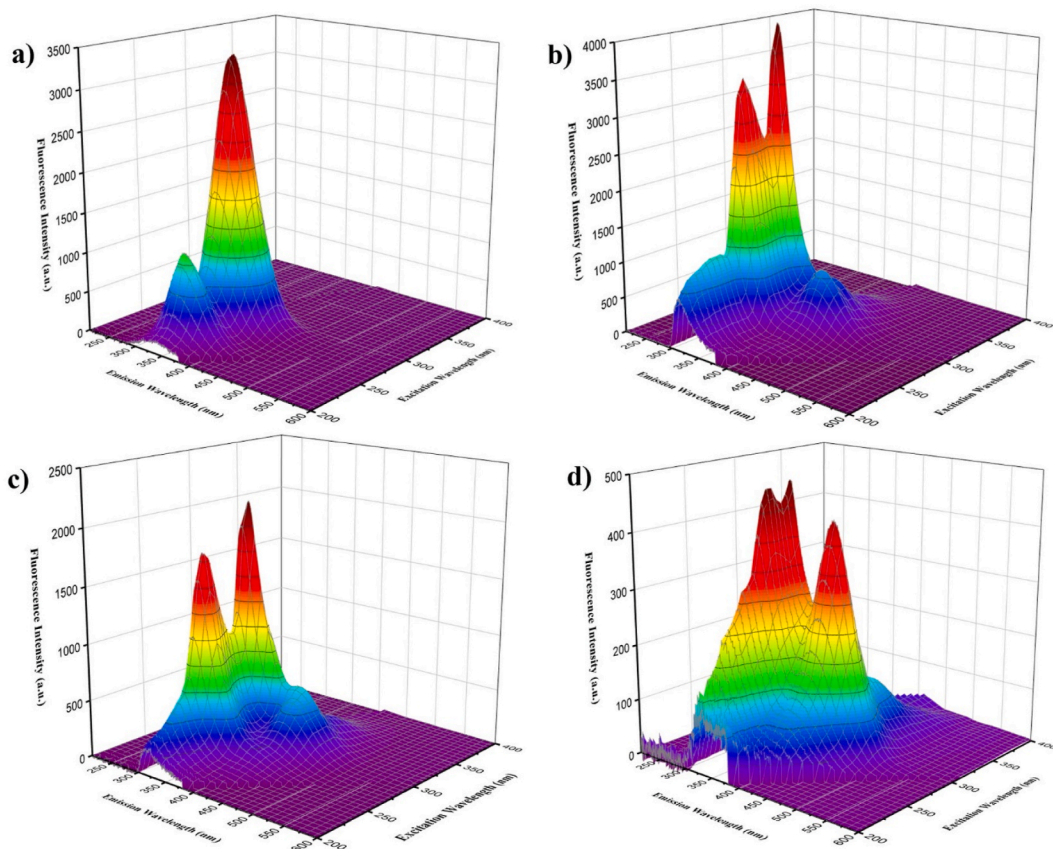


Fig. 5. Three-dimensional fluorescence spectra of BSA, a) BSA alone where $c(\text{BSA}) = 1 \text{ mg/ml}$ and its interaction of b) Eugenol Drug loaded nanoemulsion, c) Clove Drug loaded nanoemulsion, d) Cinnamon Drug loaded nanoemulsion, where the concentration $c(\text{EDLNE}) = c(\text{CLDLNE}) = c(\text{CNDLNE}) = 250 \mu\text{L}$.

scattering, in which the emission maxima (λ_{em}) and excitation maxima (λ_{ex}) are equal. Peak a showed increased intensity following contact with the nanoemulsion, verifying that BSA has aggregated onto the surface of the nanoemulsion. The system grows in size as aggregation improves, which causes the scattering mechanism to become more effective [34]. Peak 1 represents the behavior of

aromatic amino acid residues. When excited at 279 nm, the emission maxima of BSA were seen at 339 nm, as represented in Fig. 5 a. A blue shift was seen for the interacted sample, and peak maxima were shifted from 339 nm to 314 nm–325 nm. The appearance of distinct overlapping peaks observed in the interacted sample was due to their conformation changes in the secondary structure of the BSA protein as shown in Fig. 5 b for EDLNE, Fig. 5 c for CLDLNE, and Fig. 5 d for CNDLNE. Peak 2 was due to the backbone of polypeptide structures [57]. Hence, 3D spectra given below showed increased intensity (Peak a), indicating BSA aggregation and blue shift in Peak 1, which suggested conformational changes in the secondary structure.

3.2.6. FTIR spectroscopy

The secondary structure of protein plays a pivotal role in analyzing the interaction between the protein and its ligand. Through the use of FTIR analysis, the conformational shift brought by nanoemulsion upon binding to BSA was further analyzed. No significant peaks are seen in the FTIR spectra of BSA due to the PBS, which lessens or dominates the band structure as represented in Fig. 6 a. Hence, a second derivative FTIR spectrum has been derived as represented in Fig. 6 b. When nanoemulsion bound to BSA, the magnitude of the secondary structure bands increased, indicating a conformational shift. The amide portion of the spectrum exhibits a typical peak for BSA, with peaks at $1600\text{--}1690\text{ cm}^{-1}$, $1480\text{--}1575\text{ cm}^{-1}$, $1229\text{--}1301\text{ cm}^{-1}$, and 3300 cm^{-1} .

Moreover, the band at 1650 cm^{-1} , which originates from out-of-plane CN stretching and C–O stretching vibration, is characteristic of the amide I region. A vibration in the N–H bond causes amide II. The N–H or O–H stretching vibration is associated with a big feature between 3000 and 3300 cm^{-1} in the amide A region [58]. When nanoemulsion bound to BSA, the magnitude of the secondary structure bands increased, indicating a conformational shift. Given the increased sensitivity of the amide I region to the protein's secondary structure, we have carried out the second derivative of IR from a spectral range of $1600\text{--}1700\text{ cm}^{-1}$. The α -helix, β -sheets, β -turns, and random coils are attributed to the bands in $1648\text{--}1659$, $1610\text{--}1639$, $1665\text{--}1688$, and 1648 respectively.

Consequently, the α -helix was attributed to the peak at 1648 cm^{-1} and 1656 cm^{-1} of Amide II and Amide I. The β -sheets were allocated to bands ranging from 1615 to 1639 cm^{-1} in the second derivative IR of BSA [59]. Therefore, FTIR analysis indicated a conformational shift in BSA secondary structure upon interaction with nanoemulsion, and further changes in amide I and II regions suggested alterations in α -helix and β -sheets.

From all studies, it can be concluded that a strong interaction between tryptophan residues and nanoemulsion indicates the occurrence of conformational changes. However, there is a lack of quantitative results that reveal the extent of BSA interaction with nanoemulsions.

4. Conclusion

This study aims to investigate the BSA protein interaction with prepared Eugenol-based drug-loaded nanoemulsion. To perform this study, three individual Eugenol-based drug-loaded nanoemulsions, such as Cinnamon, Clove, and Eugenol oil nanoemulsion, were prepared as per the published literature. Further, the stability of the nanoemulsion was evaluated by centrifugation, heating and cooling cycles, and overnight incubation, which shows that the nanoemulsion is stable as there is no phase separation or precipitation. Additionally, dynamic light scattering was used to measure size, PDI, and zeta potential, revealing the nanoemulsion's stability. The nanodroplet size range of clove oil, Eugenol, and cinnamon oil ranged from 10 to 20 nm , and due to drug incorporation, a little increase in nanoemulsion size was observed when compared to free nanoemulsion. More importantly, homogeneity was indicated by polydispersity index (PDI) values less than 0.5 , with a small, negative zeta potential value indicating using a non-ionic emulsifier. UV–visible spectroscopy showed that the interaction with the nanoemulsion enhanced absorption intensity and a redshift, indicating structural changes. As revealed by intrinsic fluorescence spectra, interaction mostly occurred with Trp 213 in the BSA's hydrophobic

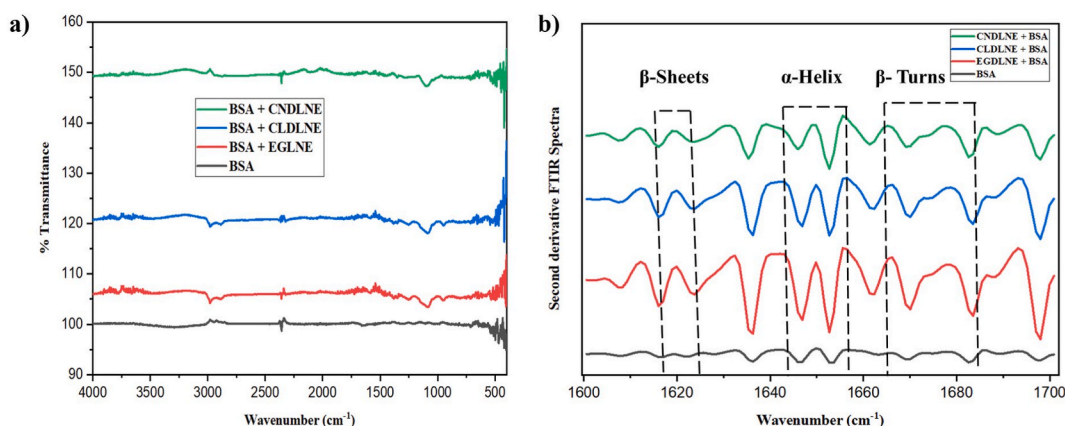


Fig. 6. FTIR spectra of BSA, $c(\text{BSA}) = 1\text{ mg/ml}$ and its interaction of Eugenol Drug loaded nanoemulsion, Clove Drug loaded nanoemulsion, Cinnamon Drug loaded nanoemulsion, where the concentration $c(\text{EDLNE}) = c(\text{CLDLNE}) = c(\text{CNDLNE}) = 250\text{ }\mu\text{L}$. a) FTIR Spectra b) Second derivative of FTIR Spectra.

pocket of domain II. Here, interaction with the nanoemulsion has a significant quenching impact on BSA, indicating structural alterations.

Additionally, strong contact with tryptophan residues was found, and synchronous spectra showed red and blue shifts, indicating changes in polarity around tryptophan and tyrosine residues. Further, increased intensity in Resonance light scattering spectra suggests that BSA aggregates on the nanoemulsion surface. Three-dimensional Fluorescence spectra and FTIR spectroscopy also revealed the conformation changes in interacting BSA with nanoemulsion, where a change in the amide I and amide II region in FTIR spectra indicates modification in α -helix and β -sheets of BSA. By analyzing all the results obtained from the experiments, we can infer that our prepared eugenol-based nanoemulsion system (Eugenol, Clove and Cinnamon) causes substantial alteration of BSA protein by losing their stability and ending with their open structure.

The study found that all the eugenol-based drug-loaded nanoemulsions significantly influenced the BSA biomolecule. This influence can be described as an initial protein stabilization, followed by a rapid and enhanced interaction with Tryptophan compared to tyrosine. Given the limited data on biomolecule interactions with nanoemulsions, understanding the toxicity of nanoemulsions and their interaction with biomolecules is crucial. Consequently, our study has paved the way for understanding how nanoemulsions interact with biomolecules. By analyzing the biosafety of the prepared nanoemulsion using Serum albumin, a transporter protein in the bloodstream, we can provide a more efficient drug delivery system by reducing toxicity. This research, therefore, holds substantial pharmacological importance in developing a safer and more precisely targeted drug delivery system with improved biosafety. The outcomes of the interaction between the blood carrier protein, BSA, and the newly developed nanoemulsion-based drug-carrier system, offer important information for developing better carriers that will cause fewer side effects in patients in the future. This is especially crucial since medications that bind to transport proteins using ligands have the potential to cause unfavorable conformational alterations. Finding safe, side-effect-free therapy options is aided by screening innovative delivery systems, such as nanoemulsion, using BSA. The effectiveness and biosafety of this therapy approach in MDR-TB patients can be strongly validated by additional research employing *in vitro* and *in vivo* models.

Data availability

Data will be made available on request.

CRedit authorship contribution statement

Keerthana M: Writing – review & editing, Writing – original draft, Methodology, Investigation, Formal analysis, Data curation. **Parvathy Mohan Menon:** Writing – original draft, Validation, Methodology, Investigation, Conceptualization. **George Priya Doss C:** Project administration, Funding acquisition. **Chandrasekaran Natarajan:** Writing – review & editing, Supervision, Resources, Project administration, Methodology, Funding acquisition, Conceptualization.

Declaration of competing interest

The authors declare that they have no known competing financial interests or personal relationships that could have appeared to influence the work reported in this paper.

Acknowledgment

This work was financially supported by the Indian Council for Medical Research (ICMR), New Delhi [Project No: 5/8/5/48/Adhoc/2022/ECD-1]. The authors were thankful to VIT University, Vellore, for providing the workplace where we could conduct our research.

References

- [1] K. Patil, S. Bagade, S. Bonde, S. Sharma, G. Saraogi, Recent therapeutic approaches for the management of tuberculosis: challenges and opportunities, *Biomed. Pharmacother.* 99 (2018) 735–745, <https://doi.org/10.1016/j.biopha.2018.01.115>.
- [2] Global Tuberculosis Report 2022, 2022. <http://apps.who.int/bookorders>.
- [3] F. Andrade, D. Rafael, M. Videira, D. Ferreira, A. Sosnik, B. Sarmento, Nanotechnology and pulmonary delivery to overcome resistance in infectious diseases, *Adv. Drug Deliv. Rev.* 65 (2013) 1816–1827, <https://doi.org/10.1016/j.addr.2013.07.020>.
- [4] R. Singh, M.S. Smitha, S.P. Singh, The role of nanotechnology in combating multi-drug resistant bacteria, *J. Nanosci. Nanotechnol.* 14 (2014) 4745–4756, <https://doi.org/10.1166/jnn.2014.9527>.
- [5] S. Banyal, P. Malik, H.S. Tuli, T.K. Mukherjee, Advances in nanotechnology for diagnosis and treatment of tuberculosis, *Curr. Opin. Pulm. Med.* 19 (2013) 289–297, <https://doi.org/10.1097/MCP.0b013e32835eff08>.
- [6] F. De Maio, V. Palmieri, G. Santarelli, G. Perini, A. Salustri, I. Palucci, M. Sali, J. Gervasoni, A. Primiano, G. Ciasca, M. Sanguinetti, M. De Spirito, G. Delogu, M. Papi, Graphene oxide-linezolid combination as potential new anti-tuberculosis treatment, *Nanomaterials* 10 (2020) 1–14, <https://doi.org/10.3390/nano10081431>.
- [7] H. Su, Y. Wang, Y. Gu, L. Bowman, J. Zhao, M. Ding, Potential applications and human biosafety of nanomaterials used in nanomedicine, *J. Appl. Toxicol.* 38 (2018) 3–24, <https://doi.org/10.1002/jat.3476>.
- [8] I. Roy, N. Vij, Nanodelivery in airway diseases: challenges and therapeutic applications, *Nanomedicine* 6 (2010) 237–244, <https://doi.org/10.1016/j.nano.2009.07.001>.
- [9] R. Duncan, R. Gaspar, Nanomedicine(s) under the microscope, *Mol. Pharm.* 8 (2011) 2101–2141, <https://doi.org/10.1021/mp200394t>.
- [10] R. Bosetti, L. Vereeck, Future of nanomedicine: obstacles and remedies, *Nanomedicine* 6 (2011) 747–755, <https://doi.org/10.2217/nmm.11.55>.
- [11] L. Zhang, D. Pornpattananankul, C.-M.J. Hu, C.-M. Huang, Development of Nanoparticles for Antimicrobial Drug Delivery, 2010.

- [12] N. Lewinski, V. Colvin, R. Drezek, Cytotoxicity of nanoparticles, *Small* 4 (2008) 26–49, <https://doi.org/10.1002/sml.200700595>.
- [13] H. Rachmawati, D.K. BudiPutra, R. Mauludin, Curcumin nanoemulsion for transdermal application: formulation and evaluation, *Drug Dev. Ind. Pharm.* 41 (2015) 560–566, <https://doi.org/10.3109/03639045.2014.884127>.
- [14] H.Y. Karasulu, Microemulsions as novel drug carriers: the formation, stability, applications and toxicity, *Expet Opin. Drug Deliv.* 5 (2008) 119–135, <https://doi.org/10.1517/17425247.5.1.119>.
- [15] H. Wang, R. Lv, S. Gao, Y. Wang, N. Hao, Y. An, Y. Li, Y. Ji, M. Cao, Investigation of the interaction between the functionalized mesoporous silica nanocarriers and bovine serum albumin via multi-spectroscopy, *Spectrochim. Acta Mol. Biomol. Spectrosc.* 293 (2023), <https://doi.org/10.1016/j.saa.2023.122421>.
- [16] C. Ge, J. Du, L. Zhao, L. Wang, Y. Liu, D. Li, Y. Yang, R. Zhou, Y. Zhao, Z. Chai, C. Chen, Binding of blood proteins to carbon nanotubes reduces cytotoxicity, *Proc. Natl. Acad. Sci. USA* 108 (2011) 16968–16973, <https://doi.org/10.1073/pnas.1105270108>.
- [17] J. Liu, T. Chu, M. Cheng, Y. Su, G. Zou, S. Hou, Bovine serum albumin functional graphene oxide membrane for effective chiral separation, *J. Membr. Sci.* 668 (2023) 121198, <https://doi.org/10.1016/j.memsci.2022.121198>.
- [18] G. Sudlow, D.J. Birkett, D.N. Wade, Further characterization of specific drug binding sites on human serum albumin, *Mol. Pharmacol.* 12 (6) (1976 Nov) 1052–1061. PMID: 1004490.
- [19] G. Sekar, A. Sivakumar, A. Mukherjee, N. Chandrasekaran, Probing the interaction of neem oil based nanoemulsion with bovine and human serum albumins using multiple spectroscopic techniques, *J. Mol. Liq.* 212 (2015) 283–290, <https://doi.org/10.1016/j.molliq.2015.09.022>.
- [20] Priyadarshini Mohapatra, Natarajan Chandrasekaran, Effects of black cumin-based antimalarial drug loaded with nano-emulsion of bovine and human serum albumins by spectroscopic and molecular docking studies, *Heliyon* 9 (1) (2023) 121198.
- [21] X. Long, Y.-F. Zeng, Y. Liu, Y. Liu, T. Li, L. Liao, Y. Guo, Synthesis of novel genistein amino acid derivatives and investigation on their interactions with bovine serum albumin by spectroscopy and molecular docking, *RSC Adv.* 8 (2018) 31201–31212, <https://doi.org/10.1039/C8RA06691D>.
- [22] P.M. Menon, N. Chandrasekaran, C. George Priya Doss, S. Shanmugam, Multi-drug loaded eugenol-based nanoemulsions for enhanced anti-mycobacterial activity, *RSC Med. Chem.* 14 (2023) 433–443, <https://doi.org/10.1039/d2md00320a>.
- [23] R. Aboofazeli, *Nanomeric-Scaled Emulsions (Nanoemulsions)*, 2010.
- [24] L. Pavoni, D.R. Perinelli, A. Ciacciarelli, L. Quassinti, M. Bramucci, A. Miano, L. Casertari, M. Cespi, G. Bonacucina, G.F. Palmieri, Properties and stability of nanoemulsions: how relevant is the type of surfactant? *J. Drug Deliv. Sci. Technol.* 58 (2018) 101772 <https://doi.org/10.1016/j.jddst.2020.101772>.
- [25] V.D. Suryawanshi, L.S. Walekar, A.H. Gore, P. V Anbhule, G.B. Kolekar, Spectroscopic analysis on the binding interaction of biologically active pyrimidine derivative with bovine serum albumin, *J Pharm Anal* 6 (2016) 56–63, <https://doi.org/10.1016/j.jpaha.2015.07.001>.
- [26] Q. Zhang, Y. Sha, J.-H. Wang, 8-Hydroxyquinoline dansylates modified with PAMAM dendrimer as fluorescent Fe³⁺ sensors, *Molecules* 15 (2010) 2962–2971, <https://doi.org/10.3390/molecules15052962>.
- [27] F. Dangkoob, M.R. Housaindokht, A. Asodeh, O. Rajabi, Z. Rouhbkahsh Zaeri, A. Verdian Doghaei, Spectroscopic and molecular modeling study on the separate and simultaneous bindings of alprazolam and flouxetine hydrochloride to human serum albumin (HSA): with the aim of the drug interactions probing, *Spectrochim. Acta Mol. Biomol. Spectrosc.* 137 (2015) 1106–1119, <https://doi.org/10.1016/j.saa.2014.08.149>.
- [28] Y. Li, Y. Zhang, S. Sun, A. Zhang, Y. Liu, Binding investigation on the interaction between Methylene Blue (MB)/TiO₂ nanocomposites and bovine serum albumin by resonance light-scattering (RLS) technique and fluorescence spectroscopy, *J. Photochem. Photobiol., B* 128 (2013) 12–19, <https://doi.org/10.1016/j.jphotobiol.2013.07.027>.
- [29] X.Y. Jiang, W.X. Li, H. Cao, Study of the interaction between trans-resveratrol and BSA by the multi-spectroscopic method, *J. Solut. Chem.* 37 (2008) 1609–1623, <https://doi.org/10.1007/s10953-008-9323-x>.
- [30] D.M. Byler, H. Susi, Examination of the Secondary Structure of Proteins by Deconvolved FTIR Spectra, n.d.
- [31] J. Kong, S. Yu, Fourier transform infrared spectroscopic analysis of protein secondary structures, *Acta Biochim. Biophys. Sin.* 39 (2007) 549–559, <https://doi.org/10.1111/j.1745-7270.2007.00320.x>.
- [32] S. Bose, A. Chatterjee, S.K. Jenifer, B. Mondal, P. Srikrishnarka, D. Ghosh, A.R. Chowdhuri, M.P. Kannan, S.V. Elchuri, T. Pradeep, Molecular materials through microdroplets: synthesis of protein-protected luminescent clusters of noble metals, *ACS Sustain. Chem. Eng.* 9 (2021) 4554–4563, <https://doi.org/10.1021/acssuschemeng.0c09145>.
- [33] M. Danaei, M. Dehghankhold, S. Ataei, F. Hasanzadeh Davarani, R. Javanmard, A. Dokhani, S. Khorasani, M.R. Mozafari, Impact of particle size and polydispersity index on the clinical applications of lipidic nanocarrier systems, *Pharmaceutics* 10 (2018), <https://doi.org/10.3390/pharmaceutics10020057>.
- [34] G. Sekar, S. Sugumar, A. Mukherjee, N. Chandrasekaran, Multiple spectroscopic studies of the structural conformational changes of human serum albumin - essential oil based nanoemulsions conjugates, *J. Lumin.* 161 (2015) 187–197, <https://doi.org/10.1016/j.jlumin.2014.12.058>.
- [35] D. Raghav, S. Mahanty, K. Rathinasamy, Characterizing the interactions of the antipsychotic drug trifluoperazine with bovine serum albumin: probing the drug-protein and drug-drug interactions using multi-spectroscopic approaches, *Spectrochim. Acta Mol. Biomol. Spectrosc.* 226 (2020), <https://doi.org/10.1016/j.saa.2019.117584>.
- [36] H. Xu, N. Yao, H. Xu, T. Wang, G. Li, Z. Li, Characterization of the interaction between eupatorin and bovine serum albumin by spectroscopic and molecular modeling methods, *Int. J. Mol. Sci.* 14 (2013) 14185–14203, <https://doi.org/10.3390/ijms140714185>.
- [37] X. Zhao, R. Liu, Z. Chi, Y. Teng, P. Qin, New insights into the behavior of bovine serum albumin adsorbed onto carbon nanotubes: comprehensive spectroscopic studies, *J. Phys. Chem. B* 114 (2010) 5625–5631, <https://doi.org/10.1021/jp100903x>.
- [38] N.M. Zadyanova, G.P. Yampol'skaya, L.Y. Filatova, Interaction of bovine serum albumin with nonionic surfactant Tween 80 in aqueous solutions: complexation and association, *Colloid J.* 68 (2006) 162–172, <https://doi.org/10.1134/S1061933X06020074>.
- [39] J. Liu, G.Y. Xu, D. Wu, L. Yu, Spectroscopic study on the interaction between bovine serum albumin and tween-20, *J. Dispersion Sci. Technol.* 27 (2006) 835–838, <https://doi.org/10.1080/01932690600719099>.
- [40] O. Soltanabadi, M.S. Atri, M. Bagheri, Spectroscopic analysis, docking and molecular dynamics simulation of the interaction of cinnamaldehyde with human serum albumin, *J. Inclusion Phenom. Macrocycl. Chem.* 91 (2018) 189–197, <https://doi.org/10.1007/s10847-018-0811-3>.
- [41] L.I. Jin-zhi, L.I.U. Chang-jin, S.H.E. Zhi-yu, Z.H.O.U. Biao, X.I.E. Zhi-yong, Z.H.A.N.G. Jun-bing, J.I.A.N.G. Shen-hua, Antiglycation activity on LDL of clove essential oil and the interaction of its most abundant component—eugenol with bovine serum albumin, *Spectrosc. Spectr. Anal.* 43 (2023) 324–332.
- [42] S.K. Chaturvedi, M.K. Siddiqi, P. Alam, M. Zaman, R.H. Khan, Comparative binding study of anti-tuberculosis drug pyrazinamide with serum albumins, *RSC Adv.* 6 (2016) 85860–85869, <https://doi.org/10.1039/c6ra10487h>.
- [43] S.A. Markarian, M.G. Aznauryan, Study on the interaction between isoniazid and bovine serum albumin by fluorescence spectroscopy: the effect of dimethylsulfoxide, *Mol. Biol. Rep.* 39 (2012) 7559–7567, <https://doi.org/10.1007/s11033-012-1590-3>.
- [44] P.A. Magdum, N.M. Gokavi, S.T. Nandibewoor, Study on the interaction between anti-tuberculosis drug ethambutol and bovine serum albumin: multispectroscopic and cyclic voltammetric approaches, *Luminescence* 32 (2017) 206–216, <https://doi.org/10.1002/bio.3169>.
- [45] S. Vallie, S. Naidoo, Identification of the binding interaction of anti-TB drugs with human serum albumin: a computational molecular docking, Fluorescence and Absorption Spectroscopy Study (2020), <https://doi.org/10.25258/ijpqa.11.1.00>.
- [46] F. Kong, S. Kang, J. Tian, M. Li, X. Liang, M. Yang, Y. Zheng, Y. Pi, X. Cao, Y. Liu, X. Yue, Interaction of xylitol with whey proteins: multi-spectroscopic techniques and docking studies, *Food Chem.* 326 (2020) 126804, <https://doi.org/10.1016/j.foodchem.2020.126804>.
- [47] D. Raghav, S. Mahanty, K. Rathinasamy, Biochemical and toxicological investigation of karanjin, a bio-pesticide isolated from Pongamia seed oil, *Pestic. Biochem. Physiol.* 157 (2019) 108–121, <https://doi.org/10.1016/j.pestbp.2019.03.011>.
- [48] P.N. Naik, S.A. Chimatadar, S.T. Nandibewoor, Interaction between a potent corticosteroid drug – dexamethasone with bovine serum albumin and human serum albumin: a fluorescence quenching and fourier transformation infrared spectroscopy study, *J. Photochem. Photobiol., B* 100 (2010) 147–159, <https://doi.org/10.1016/j.jphotobiol.2010.05.014>.
- [49] F. Ding, W. Liu, L. Zhang, B. Yin, Y. Sun, Sulfometuron-methyl binding to human serum albumin: evidence that sulfometuron-methyl binds at the Sudlow's site I, *J. Mol. Struct.* 968 (2010) 59–66, <https://doi.org/10.1016/j.molstruc.2010.01.020>.

- [50] Quenching of fluorescence, in: J.R. Lakowicz (Ed.), Principles of Fluorescence Spectroscopy, Springer US, Boston, MA, 2006, pp. 277–330, https://doi.org/10.1007/978-0-387-46312-4_8.
- [51] M. Hossain, A.Y. Khan, G. Suresh Kumar, Interaction of the anticancer plant alkaloid sanguinarine with bovine serum albumin, PLoS One 6 (2011) e18333, <https://doi.org/10.1371/journal.pone.0018333>.
- [52] O. Rinco, J. Brenton, A. Douglas, A. Maxwell, M. Henderson, K. Indrelie, J. Wessels, J. Widin, The effect of porphyrin structure on binding to human serum albumin by fluorescence spectroscopy, J. Photochem. Photobiol. Chem. 208 (2009) 91–96, <https://doi.org/10.1016/j.jphotochem.2009.08.009>.
- [53] D. Raghav, S. Mahanty, K. Rathinasamy, Characterizing the interactions of the antipsychotic drug trifluoperazine with bovine serum albumin: probing the drug-protein and drug-drug interactions using multi-spectroscopic approaches, Spectrochim. Acta Mol. Biomol. Spectrosc. 226 (2020), <https://doi.org/10.1016/j.saa.2019.117584>.
- [54] E. Sadat Mostafavi, A. Asoodeh, J. Chamani, Evaluation of interaction between Ponceau 4R (P4R) and trypsin using kinetic, spectroscopic, and molecular dynamics simulation methods, J. Mol. Liq. 362 (2022) 119761, <https://doi.org/10.1016/j.molliq.2022.119761>.
- [55] J. Mariam, P.M. Dongre, D.C. Kothari, Study of interaction of silver nanoparticles with bovine serum albumin using fluorescence spectroscopy, J. Fluoresc. 21 (2011) 2193–2199, <https://doi.org/10.1007/s10895-011-0922-3>.
- [56] N.V. dos Santos, C.F. Saponi, T.L. Greaves, J.F.B. Pereira, Revealing a new fluorescence peak of the enhanced green fluorescent protein using three-dimensional fluorescence spectroscopy, RSC Adv. 9 (2019) 22853–22858, <https://doi.org/10.1039/C9RA02567G>.
- [57] H. Yang, Y. Huang, J. Liu, P. Tang, Q. Sun, X. Xiong, B. Tang, J. He, H. Li, Binding modes of environmental endocrine disruptors to human serum albumin: insights from STD-NMR, ITC, spectroscopic and molecular docking studies, Sci. Rep. 7 (2017) 11126, <https://doi.org/10.1038/s41598-017-11604-3>.
- [58] K.A. Kristoffersen, A. van Amerongen, U. Böcker, D. Lindberg, S.G. Wubshet, H. de Vogel-van den Bosch, S.J. Horn, N.K. Afseth, Fourier-transform infrared spectroscopy for monitoring proteolytic reactions using dry-films treated with trifluoroacetic acid, Sci. Rep. 10 (2020) 7844, <https://doi.org/10.1038/s41598-020-64583-3>.
- [59] S. Bose, A. Chatterjee, S.K. Jenifer, B. Mondal, P. Srikrishnarka, D. Ghosh, A.R. Chowdhuri, M.P. Kannan, S. V. Elchuri, T. Pradeep, Molecular materials through microdroplets: synthesis of protein-protected luminescent clusters of noble metals, ACS Sustain. Chem. Eng. 9 (2021) 4554–4563, <https://doi.org/10.1021/acssuschemeng.0c09145>.